ELSEVIER

Biochimica et Biophysica Acta 1467 (2000) 406–418

BIOCHIMICA ET BIOPHYSICA ACTA
BBA

www.elsevier.com/locate/bba

A carboxy-terminal α-helical segment in the rat skeletal muscle voltage-dependent Na^+ channel is responsible for its interaction with the amino-terminus

Hui Zhang [a,1], Sylvia Kolibal [b], Jane M. Vanderkooi [a], Sidney A. Cohen [b,2], Roland G. Kallen [a,c,*]

[a] *Department of Biochemistry and Biophysics, University of Pennsylvania School of Medicine, 913B Stellar-Chance Building, 422 Curie Boulevard, Philadelphia, PA 19104-6059, USA*

[b] *Department of Medicine, University of Pennsylvania School of Medicine, Philadelphia, PA 19104, USA*

[c] *The David Mahoney Institute of Neurological Sciences, University of Pennsylvania School of Medicine, Philadelphia, PA 19104, USA*

Received 23 November 1999; received in revised form 1 May 2000; accepted 5 May 2000

Abstract

Cytoplasmic segments of the adult rat skeletal muscle sodium channel α-subunit (rSkM1) comprise a major portion (~40%) of the total protein and are involved in channel functions both general, such as inactivation, and isoform-specific, for example, protein kinase A modulation. Far ultraviolet circular dichroism measurements of synthetic peptides and overexpressed fusion proteins containing individual channel cytoplasmic segments suggest that cytoplasmic domains of rSkM1 contain ordered secondary structures even in the absence of adjoining transmembrane segments. Intrinsic fluorescence experiments with a nested set of carboxy-terminal deletion proteins confirm a specific interaction between the channel's amino- and carboxy-termini and identify residues 1716–1737 in the carboxy-terminus as the region that binds to the amino-terminus. Circular dichroism measurements suggest that this same region is organized as an α-helix and that electrostatic forces may contribute to this association. The interaction of the amino- and carboxy-termini is not accompanied by secondary structure changes detectable by circular dichroism spectroscopy, but a decrease in intrinsic fluorescence indicates that this association is accompanied by a change in the environment of Trp^{1617}.

Keywords: Sodium channel; Skeletal muscle; Overexpression; Structure; Circular dichroism; Fluorescence

Abbreviations: CD, circular dichroism; CT, carboxy-terminus; ID, interdomain; MBP, maltose binding protein; NT, amino-terminus; PAGE, polyacrylamide gel electrophoresis; rSkM1, adult rat skeletal muscle voltage-sensitive sodium channel isoform 1 (also called μ_1); SDS, sodium dodecyl sulfate; UV, ultraviolet

* Corresponding author. Fax: +1-215-573-7058; E-mail: rgk@mail.med.upenn.edu

[1] Present address: Cell Signaling Technology, Inc., 32 Tozer Road, Beverly, MA 01915, USA.

[2] Present address: Centocor, Inc., 200 Great Valley Parkway, Malvern, PA 19355-1307, USA.

0005-2736/00/$ – see front matter
PII: S0005-2736(00)00238-8

1. Introduction

The rat skeletal muscle voltage-dependent Na^+ channel isoform 1 (rSkM1)[3] protein is composed of one large α-subunit (1840 residues) and one smaller β-subunit (218 residues), but only the α-subunit is required for voltage-dependent, ion-selective function and it is this polypeptide that contains toxin binding sites [1,2]. The α-subunit consists of four domains (D1–D4) composed of 250–300 amino acids exhibiting approximately 50% homology with each other [2], and these domains are arranged around a central pore. Hydropathy analysis identifies at least six stretches of 18–25 amino acids within each domain, displaying characteristics consistent with a transmembrane helical structure (S1–S6) [2,3]. The N- and C-termini and the interdomain segments are intracellular in location [4].

A major goal of voltage-gated ion channel research is to determine the precise tertiary structure of these tetradomain proteins and to identify the factors involved in establishing and maintaining this structure [1,2]. Because efforts to ascertain the secondary and tertiary structure of large integral membrane proteins by direct methods such as X-ray diffraction, nuclear magnetic resonance (NMR) or electron microscopy have generally not been successful, recent efforts have involved direct studies of smaller recombinant protein domains or synthetic peptides [5,6] or employed other biochemical and biophysical techniques to indirectly probe membrane protein structure and topology [7–14]. These approaches have contributed detailed information regarding sodium channel secondary and tertiary structure. Previous studies involving proteolysis of both membrane-embedded and detergent-solubilized rSkM1 established the presence of four protease-resistant regions corresponding to the four homologous membrane-inserted domains and led to a model of the secondary and tertiary structure of channel cytoplasmic segments in which: (i) the amino-terminus is organized as a compact, protease-resistant structure; (ii) the exquisitely protease-sensitive carboxy-terminus is present in an extended conformation; and (iii) the other interdomain regions are composed of secondary structures between the extremes of the amino- and carboxy-termini based on their intermediate degrees of protease sensitivity [7]. Studies involving competition between antibodies for binding to purified, detergent-solubilized channel protein were able to refine this model such that: (i) the compact amino-terminus forms a rigid structure with its initial portion directed away from the bulk of the channel's cytoplasmic mass; (ii) the interdomain (ID) 2–3 region extends perpendicular to the plane of the membrane and is approximately equidistant from the remaining cytoplasmic segments; and (iii) the amino-terminus and the carboxy-terminus are intimately associated with each other [8]. Specific, high affinity complex formation was demonstrated between overexpressed amino- and carboxy-terminal segments, suggesting that these fusion proteins have defined structures that are able to faithfully mimic the interaction of these two segments within the context of the intact channel protein. The segments involved in this interaction have been identified as residues 13–30 and 1716–1737 in the channel's amino- and carboxy-termini, respectively, based on biochemical binding assays utilizing synthetic peptides and fusion proteins [9] (unpublished observations).

To test the hypothesis that the large cytoplasmic portions of the sodium channel have defined structures and to further investigate their specific interactions, bacterially overexpressed fusion proteins were examined by far ultraviolet (UV) circular dichroism (CD) and intrinsic fluorescence spectroscopy. We demonstrate that cytoplasmic domains contain regions of ordered structure even when expressed without their adjacent intramembranous domains. Far UV CD and intrinsic fluorescence studies of amino- and carboxy-terminal fusion proteins provide additional evidence for the specific interaction between sodium channel amino- and carboxy-termini and suggest that (i) no changes in secondary structure occur upon complex formation; (ii) the carboxy-terminal region involved in this interaction is organized as a short α-helix; and (iii) binding involves electrostatic interactions. Thus, these recombinant proteins

[3] The nucleotide sequence for rSkM1 has been deposited in the GenBank database under accession number M26643 [43]. The amino acid sequence of this protein can be accessed through the NCBI protein database under accession number 116453 [43].

appear to duplicate the corresponding structures and interactions present in the native protein even when devoid of the transmembrane segments.

2. Materials and methods

2.1. Materials

Chemicals and biochemicals were generally of the highest grade available and were obtained from Sigma (St. Louis, MO) or Fisher Scientific Corp. (Pittsburgh, PA). Restriction enzymes, factor X_a, and enterokinase were purchased from New England Biolabs Inc. (NEB, Beverly, MA). The expression systems pMAL-c2 and pFLAG2, were obtained from NEB and Eastman Kodak Co. (EKC, New Haven, CT), respectively. Oligopeptides were synthesized using methods detailed in earlier publications [7,8,15].

2.2. Fusion protein construct generation

The 5′- and 3′-oligonucleotide primers used to make PCR products for generating maltose binding protein (MBP) fusion proteins (at the MBP carboxy-terminus) are (restriction enzyme site underlined, 5′-primer for all carboxy-terminal constructs is sense): GAGGGAATTC**AAT**TTCAACGTGGCCACCG, channel sequence starts at **Asn**[1593]. 3′-primers (antisense): GCTCTAGA**CAC**GGTGGGTCCAGCATCC, channel sequence terminates at **Val**[1800]; GCTCTAGA**AAG**CAATCCCTCCTTCTCG, channel sequence ends at **Leu**[1765]; GCTCTAGA**GAG**GGTGGTGGTGATGGGC, channel sequence ends at **Leu**[1715]. The *Eco*RI/*Xba*I fragments were subcloned into the corresponding sites of pMAL-c2. The carboxy-terminal deletions MBP/CT1737 and MBP/CT1641 are from the *Pst*I partial digestion of PCR product CT1800, the *Eco*RI/*Pst*I fragments were cloned into the corresponding sites of pMAL-c2, and terminate at Gln[1737] and Gln[1641], respectively.

Oligonucleotide primers for making a FLAG/amino-terminal fusion proteins are (5′-primer, sense): GACGATGACAAGCTT**ATG**GCCAGCTCATCTCTG, channel sequence starts at **Met**[1]. 3′-primers (antisense): GACGATATCTCTAGA**CAC**CTTGATAGCCACCCT, channel sequence terminates at **Val**[127]; TATCTCTAGATCA**CAC**CTTGATAGCCACCCT, channel sequence terminates at **Val**[127]. Oligonucleotide primers for synthesizing the FLAG/ID3–4 fusion protein are (5′-primer, sense): GAGGAAGCTT**AAC**TTCAACCAACAGAAG, channel sequence starts at **Asn**[1290]. 3′-primer (antisense): GAGGTCTAGA**CTT**CGTCACGAAGTCG, channel sequence terminates at **Lys**[1345]. The *Hin*dIII/*Xba*I fragments were subcloned into the corresponding sites of pFLAG2.

The methods used for generating fusion proteins have been described previously [8,16]. Briefly, synthetic 5′- and 3′-oligonucleotides were used to make the PCR products for generating the MBP/carboxy-terminal, FLAG/amino-terminal and FLAG/ID3–4 fusion protein expression constructs by standard molecular cloning procedures [17]. The recombinant DNA molecules were screened by restriction enzyme digestion and the structure of each construct was confirmed by dideoxynucleotide DNA sequencing.

The carboxy-terminal fusion constructs produce protein products with 0–8 additional amino acids at the carboxy-termini as follows: MBP/Asn[1593]…Leu[1715]SRVDLQCA; MBP/Asn[1593]…Gln[1737]CA; MBP/Asn[1593]…Leu[1765]SRVDLQCA; MBP/Asn[1593]…Val[1800]SRVDLQCA; and MBP/Asn[1593]…Val[1840] (Fig. 1). Two different FLAG/NT fusion proteins were studied: the FLAG/NT′ fusion protein has 10 additional amino acids including the FLAG epitope (underlined) at the amino-terminus: MDYKDDDDKLMet[1]…Val[127], while the FLAG/NT fusion protein has 10 additional amino acid at both the N- and the C-termini: MDYKDDDDKLMet[1]…Val[127]-SRDIVDRSLE. FLAG/ID3–4 fusion protein has 10 additional amino acids at both amino- and carboxy-termini: MDYKDDDDKLAsn[1290]…Lys[1345]SRDIVDRSLE. Details of the ID1–2 and ID2–3 fusion proteins have been published previously [8,16].

2.3. Expression, purification, and analysis of fusion proteins

With the exception of FLAG/ID3–4 fusion protein, the plasmids carrying sodium channel intracellular segments in pMAL-c2 or pFLAG2 vectors direct cytoplasmic expression of fusion proteins in

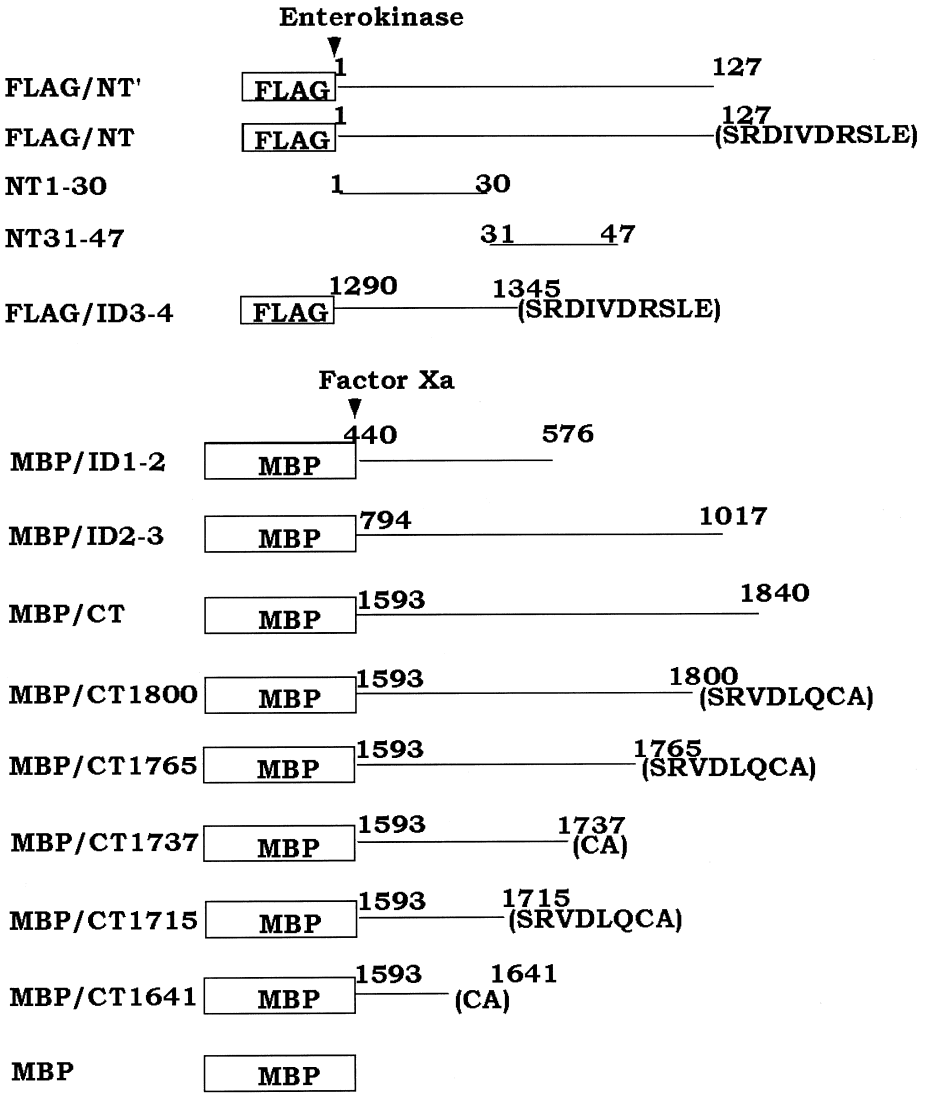

Fig. 1. MBP fusion constructs, FLAG fusion proteins, and amino-terminal synthetic peptides used in this study. Note that there is a factor X_a protease cleavage site (IEGR↓) separating MBP and sodium channel portions of the MBP fusion proteins and an enterokinase protease cleavage site (DDDDK↓) separating the FLAG epitope from the sodium channel amino-terminal sequence. Additional non-channel amino acids of the fusion proteins are indicated in parentheses.

Escherichia coli. Induction of fusion protein expression was described previously [8,16].

Cells were harvested and sonicated as published elsewhere [8]. Supernatant was collected after centrifugation at 9000×*g* at 4°C for 30 min. Fusion proteins in the supernatant were purified using amylose affinity columns (NEB) for MBP fusion proteins, or anti-M2 antibody affinity columns (EKC) for FLAG fusion protein following the manufacturers' protocols. Protein samples underwent SDS–PAGE and immunoblotting as previously described [7].

2.4. Preparation of samples for CD analysis

Samples for CD analysis were prepared in a 10 mM potassium phosphate buffer, pH 7.4 with the following protein concentrations: 2 μM MBP fusion protein, 15 μM FLAG fusion protein, and 20–50 μM amino-terminal peptides. For binding studies of sodium channel amino- and carboxy-termini, a solution of MBP/CT fusion protein (7 μM) and FLAG/NT fusion protein (20 μM) was incubated at room temperature for 2 h. An aliquot of the solution was

diluted with phosphate buffer and the CD spectrum recorded. Any dissociation in this time period is insignificant based on the previously determined dissociation rate ($t_{1/2} > 12$ h, unpublished observations). Protein concentrations of MBP fusion proteins were determined by spectrophotometric measurement of the absorption at 280 nm (Hitachi U-3000, Hitachi Scientific Instruments, Mountain View, CA) using molar absorption coefficient values [18] based on the amino acid composition of the respective protein; the protein concentrations were further confirmed by amino acid analysis (Protein Chemistry Core Facility, Columbia University, New York). The protein concentration of synthetic N-terminal peptide concentration was determined gravimetrically due to the lack of tryptophan residues in N-terminal peptides. The concentrations of both synthetic peptides and FLAG/NT were further determined by amino acid analysis.

2.5. CD spectroscopy

Far UV CD spectra were collected with a 62 DS Circular Dichroism Spectrometer (Aviv Instruments, Inc., Lakewood, NJ) using wavelengths of 185–255 nm at 25°C. The scanning speed was 6 nm/min, and the spectra were averaged (three scans). The optical path length was 1 mm. Differential CD spectra of C-terminal peptides were calculated by subtracting relevant molar normalized MBP CD spectra and converting to mean residue ellipticity, $[\theta]$ (deg cm^2 dmol^{-1}), $[\theta] = (\theta_{observed} \times 100)/(\text{mean residue concentration} \times \text{path length})$, where the $\theta_{observed}$ unit is degree, path length is in centimeters, and the mean residue concentration = number of amino acids × protein molar concentration [19].

2.6. Intrinsic fluorescence spectroscopy

To monitor the changes in the fluorescence spectrum after binding of sodium channel amino- and carboxy-termini, an aliquot of the solution containing MBP/CT fusion protein (7 μM) and FLAG/NT fusion protein (20 μM), incubated for 2 h at room temperature, was used to determine the change in fluorescence ($\lambda_{excitation} = 280$ nm, $\lambda_{emission} = 320$–520 nm) with a LS-5 fluorescence spectrophotometer (Perkin-Elmer Corp., Foster City, CA) following a 30-fold dilution immediately prior to scanning the spectrum. The scanning speed was 60 nm/min. Spectra of identical concentrations of MBP/CT fusion protein and FLAG/NT fusion protein were also recorded individually and summed in order to compare with the spectrum of the mixture.

3. Results

3.1. Bacterial expression of sodium channel cytoplasmic segments as FLAG or MBP fusion proteins

We used overexpressed, purified, recombinant MBP fusion proteins and FLAG proteins as well as synthetic peptides in this study (Fig. 1). Following purification by affinity chromatography (amylose resin for MBP fusion proteins or anti-M2 antibody affinity gel for FLAG fusion proteins), each fusion protein was identified on immunoblots developed with antibodies specific for either the encoded sodium channel segment, the FLAG epitope, or the MBP protein (Fig. 2). Anti-MBP antibody detects each of the MBP/CT fusion proteins; the migration distance of each band corresponds to that predicted from the DNA sequence (Fig. 2A). Immunoblot analysis using rSkM1 sodium channel specific polyclonal antibodies B-23 (epitope at residues 1598–1611) and I-1771 (epitope at residues 1771–1791) (Fig. 2A) demonstrates that specific immunolabeling occurs only when the fusion proteins contain the cognate epitopes, as determined from the known nucleic acid sequence. When affinity-purified FLAG/NT fusion protein was developed with anti-FLAG M2 antibody or N-terminally directed sodium channel antibody L/D3 (epitope at residues 19–24), both antibodies detected a specific protein with predicted molecular weight (Fig. 2B). Removal of the FLAG peptide from FLAG/NT fusion protein by enterokinase digestion resulted in a decrease of the amino-terminal protein size with a concomitant loss of the FLAG antibody reactivity when immunoblots were developed with sodium channel antibody L/D3 and anti-FLAG M2 antibody respectively (Fig. 2B). This demonstrates the complete removal of FLAG peptide from FLAG/NT fusion protein by enterokinase treatment. The purity of the fusion proteins was con-

firmed with Coomassie blue staining and amino acid analysis (data not shown). Each fusion protein from the affinity purification column resulted in a single major band estimated at ~90% purity.

With the exception of the fusion protein encoding the ID3–4 region, fusion proteins encoding each cytoplasmic segment were found in the soluble fraction following lysis of the transformed bacteria by sonication in the absence of detergent. Efforts to express the ID3–4 region as a FLAG fusion protein succeeded, as evidenced by a band of the expected molecular mass on Western blots of total cellular protein developed with anti-FLAG M2 antibody (not shown). We were, however, unsuccessful in purifying the protein by the standard protocol because it resides in the insoluble fraction of the bacterial lysate.

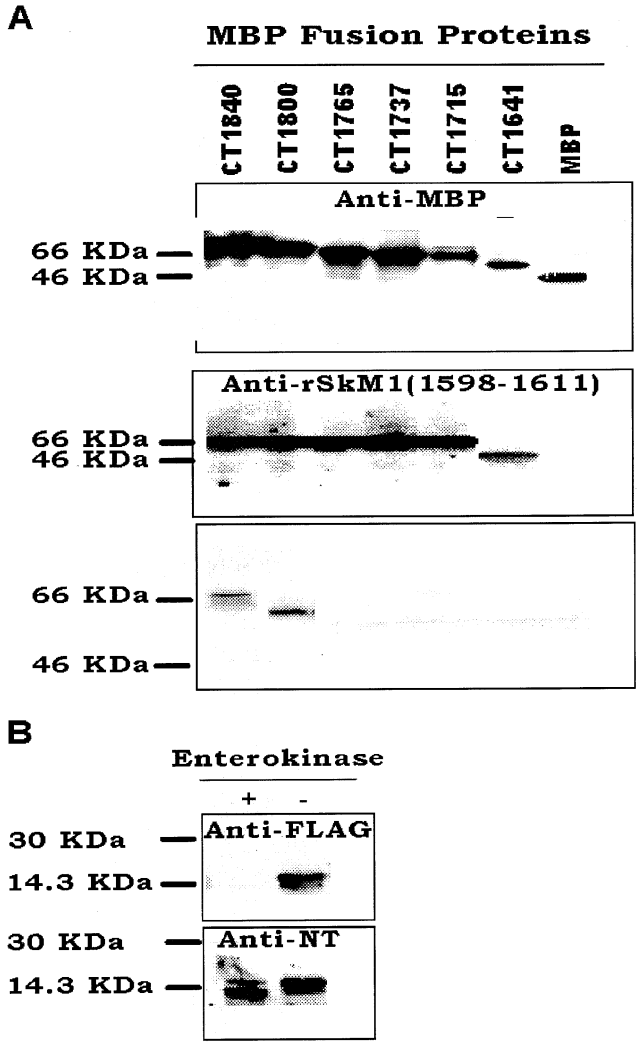

3.2. Secondary structure determination of cytoplasmic portions of sodium channel

The secondary structures of synthetic peptides and overexpressed recombinant proteins were determined by ellipticity measurements using far UV CD spectroscopy and a secondary structure analysis algorithm ([19], Table 1). Our analysis assumes that protein structure is determined by local factors and not by interactions with distant elements (i.e., secondary structure is not determined by tertiary structure or by interactions with the membrane phase). We were concerned that either the FLAG epitope or the MBP portion might alter the structure of the sodium channel segments in the fusion proteins and this was tested by looking for a change in the CD spectra of the MBP or FLAG fusion proteins before and after factor X_a or enterokinase cleavage and of the amino-terminal protein before and after cleavage (not shown). In both circumstances no change was observed, an observation that gives us confidence that neither the MBP protein nor the FLAG segment affected the spectra obtained from each of the rSkM1 cytoplasmic segment fusion proteins. Furthermore, we observed that the molar ellipticity of each of

←

Fig. 2. Immunoblots of MBP/CT and FLAG/NT fusion proteins. MBP/CT fusion proteins encoding the full-length and nested fragments of the rSkM1 carboxy-terminus (A) and FLAG/NT fusion proteins (B) were separated with SDS–PAGE and transferred to nitrocellulose, and then incubated with the indicated antibodies. The antibodies used to identify the carboxy-terminal deletion fusion proteins are: rabbit polyclonal anti-MBP antibody (A, upper); rabbit polyclonal antibody B-23 directed against residues 1598–1611 in the rSkM1 sodium channel sequence (A, middle); and rabbit polyclonal antibody I-1771 directed against residues 1771–1791 in the rSkM1 sodium channel sequence (A, lower). The antibodies used to identify the FLAG/NT fusion protein are: mouse monoclonal anti-FLAG M2 antibody (B, upper); mouse monoclonal antibody L/D3 directed against residues 19–24 in the rSkM1 amino-terminal sequence (B, lower). Treatment with enterokinase cleaves the FLAG epitope from the FLAG/NT fusion protein when immunoblots are developed with anti-FLAG M2 antibody (B, upper panel) and decreases the size of the amino-terminal protein when immunoblots are developed with L/D3 (B, lower panel). The estimated molecular mass of each band corresponds to that expected based on the DNA sequence. Specific immunolabeling occurs only when the fusion proteins contain the cognate epitope.

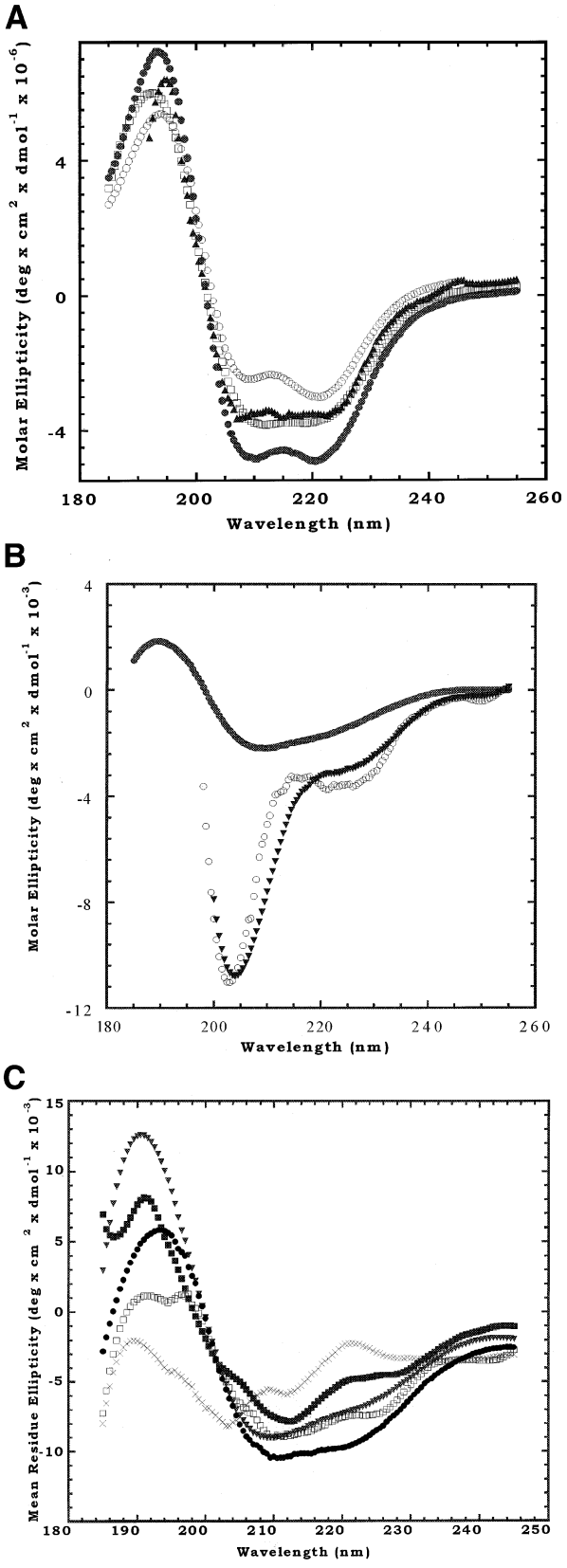

Fig. 3. CD spectra of proteins. CD spectra of MBP fusion proteins, FLAG protein, and synthetic peptides were obtained. The number of spectra which were averaged to produce these data are indicated in parentheses. (A) Molar ellipticity of MBP or MBP fusion proteins: ○ MBP (3), ▲ MBP/ID1–2 (3), ● MBP/ID2–3 (3), □ MBP/CT (3) (without subtracting the molar ellipticity of MBP). (B) Molar ellipticity of ● FLAG/NT (5), ▼ peptide NT1–30 (3), and ○ NT31–47 (3). (C) The mean residue ellipticity of carboxy-terminal deletion proteins is calculated by subtracting the molar ellipticity of MBP from the molar ellipticity of MBP/CT fusion protein and then dividing by the number of residues in each protein: ■ CT (3), ▼ CT1800 (3), ● CT1765 (4), □ CT1737 (4), × CT1715 (3).

→

the MBP sodium channel cytoplasmic fusion proteins is larger than that of the MBP 'carrier' alone (Fig. 3A). This is possible only if the sodium channel segment of the fusion protein contains secondary structures that contribute to the overall CD signal. We note that the original FLAG amino-terminal protein (FLAG/NT) contained an additional 10 residues in the end of the C-terminus. To ensure that this sequence did not significantly change the CD measurements, we constructed a second FLAG amino-terminal protein lacking this 10 residue sequence (FLAG/NT′). No significant change in predicted secondary structure was observed when the two FLAG amino-terminal proteins were compared (data not shown), consistent with the view that each of the sodium channel segments is organized as a domain distinct from the FLAG, MBP or extra flanking portions of the fusion proteins.

Although CD is most precise in estimating α-helical content [20–22], estimates of β-strand, β-turn, and random coil can be made ([19], Table 1). The CD spectra obtained with each of the four cytoplasmic segments suggest that each segment contains a significant amount of ordered structure. In these segments, between 62% and 72% of the residues are calculated to be present either as an α-helix, β-strand, or β-turn while only 28–37% of the residues are predicted to be present as a random coil. Except for the ID2–3 segment, the most dominant organized structure in these cytoplasmic segments is computed to be β-strand (55–69%) while α-helical content is estimated at 3–10%.

Of the cytoplasmic segments, the amino-terminus stands out from the three others by containing the most β-strand, the least α-helix, and no detectable

β-turn structure. Almost 70% of the amino-terminal protein is predicted to be in a β-strand conformation with only 28%, the lowest of all the segments, present as a random coil. Synthetic amino-terminal peptides encoding residues 1–30 and 31–47 also possess a secondary structure that appears to be mostly β-sheet (Fig. 3B, Table 1).

The results for the ID2–3 region contrast strongly with those for the amino-terminus (Table 1): it contains the highest α-helical content (22%), the lowest β-strand content (21%), and the highest β-turn content (19%). The ID1–2 segment resembles the amino-terminus more than the other channel segments in its secondary structure predictions: 7% α-helical content, 56% β-strand content, and 35% random coil.

Given our model of the carboxy-terminus as possessing the least compact structure, based on its marked sensitivity to proteolysis [7], we were surprised to find that the MBP carboxy-terminal fusion protein had no unique attributes with regard to any of the predicted structures: α-helical content was midway between the values for amino-terminal and ID2–3 proteins, and β-strand, β-turn, and random coil contents were also intermediate (Table 1). We were, however, able to determine the region containing α-helical secondary structure in the carboxy-terminus using CD spectroscopy and the nested set of carboxy-terminal deletion proteins (Fig. 3C). Both

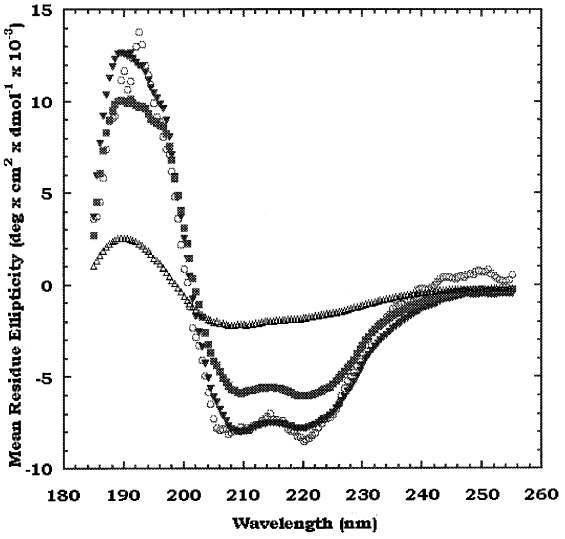

Fig. 4. CD spectra of amino- and carboxy-terminal proteins. CD spectra of the amino-terminal and carboxy-terminal proteins alone and after complex formation. CD spectra of FLAG/NT (△), MBP/CT (■), and mixture of FLAG/NT and MBP/CT (○, measured), compared to the calculated sum of FLAG/NT and MBP/CT (▼). In this set of spectra, the contribution of MBP to the CD spectra has not been subtracted.

percent α-helical content and the absolute number of residues predicted to be present as α-helix dropped to near zero when residues 1716–1737 were eliminated from the recombinant protein (Fig. 3C, Table 1). This region corresponds to the car-

Table 1
Secondary structure of cytoplasmic segments of rSkM1

Channel segment	Size (number of residues)	% α-Helix	% β-Strand	% β-Turn	% Random coil
N-terminus[a]	**147**	**3 ± 2**[b]	**69**	**0**	**28**
NT1–30	30	2 ± 3	50	5	43
NT31–47	17	2 ± 1	57	4	37
ID1–2	**137**	**7 ± 5**	**56**	**2**	**35**
ID2–3	**224**	**22 ± 2**	**21**	**19**	**37**
C-terminus	**248**	**10 ± 3**	**55**	**2**	**33**
CT1800	208	14 ± 4	56	0	30
CT1765	173	21 ± 3	23	22	35
CT1737	145	15 ± 4	29	20	36
CT1715	123	1 ± 1	55	6	37

Samples for CD analysis were prepared in a 10 mM potassium phosphate buffer, pH 7.4. Far UV CD spectra were collected using wavelengths of 185–255 nm at 25°C and the spectra were averaged (three scans). Mean residue ellipticity ([θ]) of synthetic peptides and overexpressed recombinant proteins was calculated from ellipticity measurements, $\theta_{observed}$. [θ] (deg cm^2 dmol^{-1}) = ($\theta_{observed} \times 100$)/(mean residue concentration × path length), where the $\theta_{observed}$ unit is degree, path length is in centimeters, and the mean residue concentration = number of amino acids × protein molar concentration [19]. The percentage of secondary structure was predicted using mean residue ellipticity ([θ]) and a secondary structure analysis algorithm [19].

[a] FLAG/NT (see Fig. 1).

[b] Mean ± S.D.

boxy-terminal segment found to specifically interact with the rSkM1 amino-terminus in direct binding experiments [9] (unpublished experiments).

3.3. Studies of the secondary structure involving the interactions between amino- and carboxy-termini with CD

We have modeled the amino-terminus as a rigid, compact structure based on proteolysis [7] and antibody competition data [8]. While our results suggest that the amino-terminus has significant β-strand content (~69%), which could achieve a compact structure, another possibility is that the amino-terminus assumes a more highly ordered structure only upon binding to the carboxy-terminus. Therefore, we examined whether any secondary structural changes are associated with this binding reaction. CD spectra from 185 to 255 nm, a region in which one can obtain statistically significant estimates of changes in secondary structure, were obtained from aliquots of solutions containing FLAG/NT fusion protein, MBP/CT fusion protein, or mixtures of the two proteins under conditions that allow binding of these two channel segments. Mixtures of these two proteins gave rise to CD spectra that were identical to those obtained by summing the individual spectra of the amino-terminal and carboxy-terminal proteins (Fig. 4), indicating that no detectable change in secondary structure occurs upon complex formation.

3.4. Fluorescence intensity studies reveal structural changes involved in the interaction between the amino- and carboxy-termini

A single tryptophan (Trp^{1617}) in the carboxy-terminal portion of the sodium channel is available to act as a unique intrinsic fluorophore, with a change in fluorescence intensity reporting any changes in the immediate environment of the fluorophore. The five tyrosine residues (residue 2 in the FLAG epitope and residues 68, 86, 87 and 112 in the rSkM1 amino-terminus) in the FLAG amino-terminal protein, which is devoid of tryptophan residues, would make only a small contribution to intrinsic fluorescence (Fig. 5). Although there are eight tryptophan residues in MBP protein, we first determined in a control experiment that there are no changes in fluo-

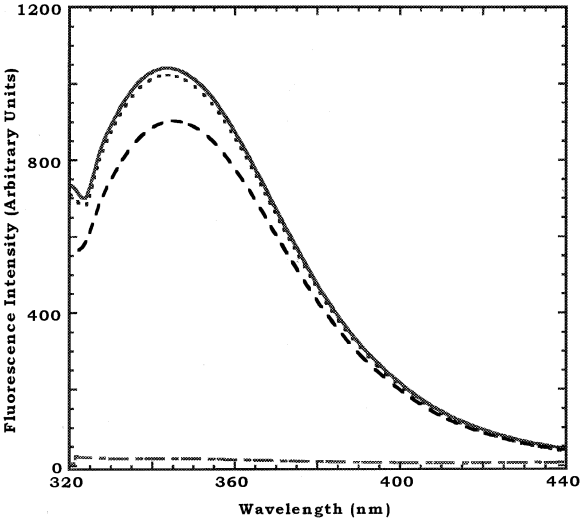

Fig. 5. Intrinsic fluorescence change due to complex formation. Fluorescence intensity spectra of FLAG/NT (0.67 mM), MBP/CT1800 (0.23 mM), and mixtures of the same concentration of the two proteins were obtained. The fluorescence intensity of carboxy-terminal Trp^{1617} is decreased after mixing FLAG/NT (dot-dashed line) with MBP/CT1800 (dashed line) compared to the fluorescence intensity of MBP/CT1800 alone (dotted line), or to the calculated sum (solid line) of fluorescence obtained individually with FLAG/NT and MBP/CT1800. FLAG/NT alone does not contribute to the fluorescence intensity.

Table 2
Decrement in relative fluorescence intensity at 342 nm after mixing MBP/CT fusion proteins with FLAG/NT

Protein	MBP	MBP/CT1800	MBP/CT1765	MBP/CT1737	MBP/CT1715
Fluorescence decrement (arbitrary units)	11.5	143.1	101.1	97.7	23.1

MBP/CT fusion protein (0.23 mM), FLAG/NT fusion protein (0.67 mM), or the mixture of identical concentration of MBP/CT and FLAG/NT fusion proteins were prepared in a 10 mM potassium phosphate buffer, pH 7.4. The fluorescence spectra of the proteins were recorded ($\lambda_{excitation} = 280$ nm, $\lambda_{emission} = 320$–520 nm) with the scanning speed of 60 nm/min at room temperature. Fluorescence spectra for the amino- or carboxy-terminal proteins separately were compared with spectra obtained with mixtures of these proteins. The values are the sum of the individual spectra of amino- and carboxy-termini minus the spectrum of the solution that contains a mixture of the same concentration of amino- and carboxy-terminal proteins.

rescence intensity of the MBP tryptophan residues upon mixing the N-terminal fusion protein with MBP protein alone. Then, fluorescence spectra from 320 to 520 nm for the amino- or carboxy-terminal proteins, recorded separately and summed, were compared with spectra obtained with mixtures of these proteins under conditions that permit complex formation (Fig. 5). Each representative of the nested set of MBP/CT fusion proteins, when mixed with the FLAG/NT fusion protein, produced a decrease in fluorescence intensity at 342 nm with the exception of MBP/carboxy-terminal fusion protein encoding residues 1593–1715 (Table 2). As noted, the MBP protein devoid of rSkM1 sequence also reveals no change in fluorescence intensity when mixed with the FLAG/NT fusion protein. The lack of fluorescence intensity change with MBP or MBP/CT1715 fusion proteins indicates that a change in the environment of the reporter Trp^{1617} in sodium channel carboxy-terminal occurs during binary complex formation between the amino- and carboxy-terminal proteins and that it is residues 1716–1737 in the carboxy-terminus that provide most of the binding site for the amino-terminus.

4. Discussion

Because of difficulties in obtaining sufficient amounts of purified native sodium channel protein for crystallization and X-ray diffraction structural studies, we and others have turned to biophysical examination of recombinant proteins or synthetic peptides to gain insight into the structure and function of specific sodium channel segments [7–14,23,24]. CD measurements of various sodium channel segments other than cytoplasmic segments reported in this study show organized secondary structures with random coil contents similar to those measured in the present study ($\sim$30%). For example, these prior studies have led to estimates of an α-helical structure for the transmembrane segments in various domains [10,23,24], predominantly α-helical and β-sheet structures for the P regions [11,12,24], a significant stretch of α-helical structure in the ID3–4 region [5,13,25], and predominantly α-helical content in the S4–S5 segments of each domain [10,14]. It is quite reassuring that CD predictions in the case of the ID3–4 region have been confirmed by 2D NMR solution structures [5,13].

Cytoplasmic segments of voltage-dependent sodium channels comprise 40–50% of the total α-subunit protein mass [2,4], contribute both conserved and diverse regions among different isoforms that account for both general (inactivation) and isoform-specific functions (ID1–2 loop-localized protein kinase A (PKA) modulation of expressed neuronal and cardiac sodium channels [26–33], which is not seen in SkM1 channels [27,33]). Increases (cardiac [31–33]) and decreases (neuronal [30]) in current amplitude have been reported in response to PKA stimulation. These cytoplasmic regions also provide possible sites for interaction with other membrane or cytoplasmic proteins that control the location of channels in the cell (e.g., localization to the neuromuscular junction). Thus, the C-termini of rSkM1 and rSkM2 contain PDZ domains [34] that are thought to interact with syntrophins (peripheral membrane proteins of the dystrophin-associated protein complex located on the cytoplasmic face of plasma membranes [35,36]). Although the removal of most of each terminus of the rat brain II isoform was associated with normal sodium currents, the channel expression level was much lower than that of the wild-type suggesting that maturation of the protein or efficiency of insertion into the membrane may be influenced by the presence and nature of cytoplasmic segments [37]. In this regard it may be relevant that K^+ channel subunit proteins are assembled into functional tetramers, and that subunit assembly is critically driven by a conserved, self-tetramerizing sequence in the N-terminal cytoplasmic region (tetramerization 1 domain) [38].

We report here the first secondary structure predictions performed on the amino-terminus, the carboxy-terminus, and the ID1–2 and 2–3 regions. To probe the structure of each sodium channel cytoplasmic segment, we overexpressed these regions as fusion proteins and studied their structures and interactions by far UV CD and fluorescence spectroscopy. With the exception of the ID3–4 protein, each of the fusion proteins was found in the soluble fraction following lysis of transformed bacteria. This observation suggests that each cytoplasmic segment is capable of forming secondary structures in the absence of either the membrane phase or other channel seg-

ments [39]. On the other hand, the FLAG/ID3–4 fusion protein was insoluble despite the fact that it contains 34 polar or charged residues out of a total of 56 residues (amino acids 1290–1345)[4]. If the ID3–4 segment is truly located in the cytoplasm in vivo, there may be a requirement for association with another part of the sodium channel in order for it to attain its physiological location (e.g., an interaction between the ID3–4 segment and the S4–S5 loop of domain 4 [40]).

The CD data for each of the soluble channel cytoplasmic segments indicate that they possess significant amounts of secondary structure (62–72%) (Table 1). Except for the ID2–3 region, each segment contains at least 50% β-strand content while the ID2–3 region contains near equal amounts of both α-helix and β-strand structures. Note that X-ray diffraction studies of the 389 residue MBP have shown it to be a compact protein with ∼40% α-helix and ∼20% β-sheet structure, consistent with our CD measurements [41]. Thus, we were able to simply subtract the contribution of the MBP carrier from the total signal obtained with the MBP fusion proteins (Fig. 3C). The short length of the FLAG segment (eight residues) limited our ability to perform the same type of correction with the FLAG/NT protein, but surely this contribution would be negligible, commensurate with its size. A comparison of CD spectra before and after factor X_a-mediated cleavage (for MBP fusion proteins, not shown) or enterokinase treatment (for the FLAG amino-terminal protein, not shown) revealed no significant differences, suggesting that the sodium channel segments do not influence MBP and FLAG structures and, presumably, vice versa. A second FLAG amino-terminal protein in which the 10 residues at the end of FLAG/NT were removed by recombinant DNA techniques to resemble more accurately the channel N-terminus yielded virtually identical secondary structure estimates compared with the original FLAG protein, increasing our confidence that any differences in structure between the overexpressed proteins and that portion of the native channel are minor and likely to be unimportant. The most important observation is that the molar ellipticity of each of the MBP sodium channel fusion proteins is larger than that of the MBP 'carrier' alone (Fig. 3A), indicating that sodium channel extramembranous portions contained in the fusion proteins are organized into specific and discrete secondary structures.

Our previous proteolysis and antibody competition studies led to a model of the structure of channel cytoplasmic segments. Some of the general features of this model are supported by the structural predictions of the present study and some of the findings in this paper advance specific aspects of this model. For example, our present observation that the amino-terminus is the most ordered of the cytoplasmic segments is consistent with the model of the amino-terminus as a compact, rigid structure. The high β-strand content (69%) and presence of multiple proline residues in the amino-terminus suggests a more detailed model in which this region contains multiple antiparallel β-sheets that interact with one another, giving rise to the compact, rigid, relatively protease-resistant structure. While our CD spectra do not provide evidence for any alteration of secondary structure as the result of complex formation between the N- and C-termini (see below), it could be the case that the N-terminus interaction with the C-terminus creates steric hindrance of the approach of protease perhaps contributing another factor, besides the intrinsic secondary structure itself, to the protease resistance of the amino-terminal segment.

The predicted secondary structures of the remaining cytoplasmic segments are not as readily rationalized. While it is tempting to suggest that the high α-helical content of the ID2–3 region is consistent with our model of this segment as projecting away from the plane of the membrane in an extended conformation, the near equal amounts of α-helical, β-sheet, and random coil contents do not lead to a simple structural model. Similarly, while our findings suggest intermediate degrees of structure for the ID1–2 and carboxy-terminal regions, it is, once again, difficult to correlate these data with a specific overall structural model. However, differences in protease sensitivity, which is greatest for the carboxy-terminus, may be due more to unencumbered cytoplasmic segment availability to soluble protease rather than to any specific secondary structural motifs.

Competition between antibodies directed against

[4] ID3–4 is conventionally defined as amino acids 1292–1344 in rSkM1.

the proximal amino-terminal and distal carboxy-terminal segments led to the suggestion that these two channel segments bind to one another [8]. Using a soluble adsorption assay, expressed amino-terminal and carboxy-terminal portions of the sodium channel were shown to bind to each other at micromolar concentrations in vitro [8]. The residues involved in the interaction are now localized to amino acids 1716–1737 in the carboxy-terminus and 13–30 in the amino-terminus (Tables 1 and 2) [9]. The fact that there are no changes in CD spectra and only a small decrease in intrinsic fluorescence upon binary complex formation supports the view that no substantial structural change is associated with the amino- and carboxy-terminus interaction.

Our studies with MBP fusion proteins containing a nested set of deletions in the carboxy-terminus have provided a tool to localize the α-helical segment in the carboxy-terminus. All of the carboxy-terminal fusion proteins, save one (CT1715) contained measurable α-helical content. The most straightforward explanation for the loss of α-helix upon deletion of the 1716–1765 segment is that the α-helix is located within this stretch of amino acids. Whether or not the apparent increase in α-helical content seen for MBP/CT1765 indicates some inhibition of α-helix formation by the presence of the distal carboxy-terminal segment (residues 1766–1800), it is clear from these data that the 1766–1840 segment contributes little, if any, α-helical content of its own.

We utilized the presence of the unique Trp^{1617} in the carboxy-terminus and the absence of tryptophan residues in the amino-terminus to assess whether any structural changes are associated with the binding reaction. Upon excitation at 280 nm, 90% of protein fluorescence is due to tryptophan (tyrosine contributes little or undetectable intrinsic fluorescence in proteins) and the tryptophan fluorescence intensity is highly sensitive to the surrounding environment [18]. Upon binding of the amino-terminal and carboxy-terminal proteins, we observed a decrease in fluorescence intensity. This decrease of fluorescence intensity may be caused by the quenching of tryptophan fluorescence by other residues that are brought into proximity with Trp^{1617} due to the interaction of the amino- and carboxy-termini. Cys^{16} in the amino-terminal segment is a reasonable candidate for this role due to its close proximity to the amino-terminal interaction surface (residues 13–30), although other side chains in the carboxy-terminus might also induce quenching if the tertiary structure of the carboxy-terminus were to change upon complex formation. However, as noted above, the observation that the CD spectrum of mixtures of amino- and carboxy-terminal proteins does not differ when compared with the summed spectrum of amino-terminal and carboxy-terminal proteins suggests that there are no major changes in secondary structure upon binary complex formation (Fig. 4). Because changes in intrinsic fluorescence were observed only when the α-helical 1716–1737 segment was present, these data provide experimental evidence that these residues form the site in the carboxy-terminal segment that interacts with the amino-terminus.

The co-localization of both binding and α-helix to the 1716–1737 segment suggests that the α-helix may contribute to the interaction surface responsible for the amino- and carboxy-terminal association. Residues 1716–1737, when viewed using a Schiffer–Edmundson helical wheel projection, present one face with four positively charged residues that would be ideally suited for interaction with amino-terminal peptide 13–30, which itself possesses two negatively charged residues separated by five residues. Thus, we propose that the middle portion of the carboxy-terminus (residues 1716–1737) interacts with the amino-terminus through electrostatic forces. We further postulate that this interaction brings Trp^{1617} and Cys^{16} together, giving rise to intrinsic fluorescence quenching. Such an interaction in the native channel could contribute to higher-order interdomain organization, that is, whether the four domains are arranged clockwise or counter-clockwise when viewed from the extracellular surface [42]. It also might determine the rapidity with which the assembly of this structure occurs.

Acknowledgements

We thank Drs. Robert L. Barchi and Weijing Sun for helpful discussions and for providing plasmid constructs containing the interdomain 1–2, interdomain 2–3, and carboxy-terminus segments. This study was supported by the National Institutes of Health Grants AR41,762 (R.G.K.), the American

Heart Association (R.G.K., S.K., S.A.C., H.Z.), the University of Pennsylvania Research Foundation (R.G.K.), the Muscular Dystrophy Association (R.G.K.) and Department of Veterans Affairs (S.A.C.).

References

[1] E. Marban, T. Yamagishi, G.F. Tomaselli, J. Physiol. 508 (1998) 647–657.
[2] R.G. Kallen, S.A. Cohen, R.L. Barchi, Mol. Neurobiol. 7 (1993) 383–428.
[3] S.D. Kraner, G.N. Filatov, W. Sun, P. Bannerman, J. Lindstrom, R.L. Barchi, J. Neurochem. 70 (1998) 1628–1635.
[4] H.A. Fozzard, D.A. Hanck, Physiol. Rev. 76 (1996) 887–926.
[5] C.A. Rohl, F.A. Boeckman, C. Baker, T. Scheuer, W.A. Catterall, R.E. Klevit, Biochemistry 38 (1999) 855–861.
[6] C. Antz, M. Geyer, B. Fakler, M.K. Schott, H.R. Guy, R. Frank, J.P. Ruppersberg, H.R. Kalbitzer, Nature 385 (1997) 272–275.
[7] S.J. Zwerling, S.A. Cohen, R.L. Barchi, J. Biol. Chem. 266 (1991) 4574–4580.
[8] W. Sun, R.L. Barchi, S.A. Cohen, J. Biol. Chem. 270 (1995) 22271–22276.
[9] H. Zhang, S. Kolibal, C. Brady, W. Sun, S.A. Cohen, Biophys. J. 70 (1996) A66.
[10] M. Brullemans, O. Helluin, J.Y. Dugast, G. Molle, H. Duclohier, Eur. Biophys. J. 23 (1994) 39–49.
[11] Y. Pouny, Y. Shai, Biochemistry 34 (1995) 7712–7721.
[12] P. Cosette, L. Brachais, E. Bernardi, H. Duclohier, Eur. Biophys. J. 25 (1997) 275–284.
[13] W. Beck, G. Jung, W.G. Bessler, I. Benz, M. Kohlhardt, Biochim. Biophys. Acta 1206 (1994) 263–271.
[14] O. Helluin, J. Breed, H. Duclohier, Biochim. Biophys. Acta 1279 (1996) 1–4.
[15] S. Kraner, J. Yang, R. Barchi, J. Biol. Chem. 264 (1989) 13273–13280.
[16] W. Sun, S.A. Cohen, R.L. Barchi, Anal. Biochem. 226 (1995) 188–191.
[17] J. Sambrook, E.F. Fritsch, T. Maniatis, Molecular Cloning: A Laboratory Manual, 2nd edn., Cold Spring Harbor Laboratory Press, Cold Spring Harbor, NY, 1989.
[18] J.R. Lakowicz, Principles of Fluorescence Spectroscopy, Plenum Press, New York, 1983.
[19] J.T. Yang, C.S. Wu, H.M. Martinez, Methods Enzymol. 130 (1986) 208–269.
[20] W.C. Johnson Jr., Annu. Rev. Biophys. Chem. 17 (1988) 145–166.
[21] W.C. Johnson Jr., Proteins 7 (1990) 205–214.
[22] W.C. Johnson Jr., Methods Enzymol. 210 (1992) 426–447.
[23] D.G. Doak, D. Mulvey, K. Kawaguchi, J. Villalain, I.D. Campbell, J. Mol. Biol. 258 (1996) 672–687.
[24] H. Duclohier, O. Helluin, P. Cosette, S. Bendahhou, Biosci. Rep. 18 (1998) 279–286.
[25] Y. Kuroda, Y. Maeda, K. Miyamoto, K. Tanaka, K. Kanaori, A. Otaka, N. Fujii, T. Nakagawa, Biophys. J. 77 (1999) 1363–1373.
[26] M.E. Gellens, A.L. George Jr., L.Q. Chen, M. Chahine, R. Horn, R.L. Barchi, R.G. Kallen, Proc. Natl. Acad. Sci. USA 89 (1992) 554–558.
[27] R.D. Smith, A.L. Goldin, J. Neurosci. 16 (1996) 1965–1974.
[28] R.D. Smith, A.L. Goldin, J. Neurosci. 17 (1997) 6086–6093.
[29] R.D. Smith, A.L. Goldin, Am. J. Physiol. 263 (1992) C660–C666.
[30] A.R. Cantrell, R.D. Smith, A.L. Goldin, T. Scheuer, W.A. Catterall, J. Neurosci. 17 (1997) 7330–7338.
[31] W. Schreibmayer, B. Frohnwieser, N. Dascal, D. Platzer, B. Spreitzer, R. Zechner, R.G. Kallen, H.A. Lester, Receptors Channels 2 (1994) 339–350.
[32] B. Frohnwieser, L. Weigl, B. Spreitzer, R.G. Kallen, W. Schreibmayer, Biophys. J. 68 (1995) A49.
[33] B. Frohnwieser, L.-Q. Chen, R.G. Kallen, W. Schreibmayer, J. Physiol. 498 (1997) 309–318.
[34] J.H. Morais Cabral, C. Petosa, M.J. Sutcliffe, S. Raza, O. Byron, F. Poy, S.M. Marfatia, A.H. Chishti, R.C. Liddington, Nature 382 (1996) 649–652.
[35] S.H. Gee, R. Madhavan, S.R. Levinson, J.H. Caldwell, R. Sealock, S.C. Froehner, J. Neurosci. 18 (1998) 128–137.
[36] J. Schultz, U. Hoffmuller, G. Krause, J. Ashurst, M.J. Macias, P. Schmieder, J. Schneider-Mergener, H. Oschkinat, Nature Struct. Biol. 5 (1998) 19–24.
[37] W. Stuhmer, F. Conti, H. Suzuki, X.D. Wang, M. Noda, N. Yahagi, H. Kubo, S. Numa, Nature 339 (1989) 597–603.
[38] N.V. Shen, X. Chen, M.M. Boyer, P.J. Pfaffinger, Neuron 11 (1993) 67–76.
[39] G.W. Abbott, M. Bloemendal, I.H. Van Stokkum, E.A. Mercer, R.T. Miller, S. Sewing, M. Wolters, O. Pongs, S.K. Srai, Biochim. Biophys. Acta 1341 (1997) 71–78.
[40] L. Tang, R.G. Kallen, R. Horn, J. Gen. Physiol. 108 (1996) 89–104.
[41] J.C. Spurlino, G.Y. Lu, F.A. Quiocho, J. Biol. Chem. 266 (1991) 5202–5219.
[42] N. Chang, G. Lipkind, H. Fozzard, J. Penzotti, A. Sunami, R. French, S. Dudley, Biophys. J. 76 (1999) A261.
[43] J.S. Trimmer, S.S. Cooperman, S.A. Tomiko, J.Y. Zhou, S.M. Crean, M.B. Boyle, R.G. Kallen, Z.H. Sheng, R.L. Barchi, F.J. Sigworth, Neuron 3 (1989) 33–49.